AD NUMBER
AD525116
LIMITATION CHANGES
TO: **Approved for public release; distribution is unlimited.**
FROM: **Distribution authorized to U.S. Gov't. agencies and their contractors; Administrative/Operational Use; 10 APR 1973. Other requests shall be referred to Naval Air Development Center, Warminister, PA 18974.**
AUTHORITY
NAWCAD memo dtd 22 Feb 2017

Cut 3438

~~CONFIDENTIAL~~

U 152017

UNCLASSIFIED

COPY 29

NAVAL AIR DEVELOPMENT CENTER

WARMINSTER, PA. 18974

REPORT NO. NADC-72167-AE 10 APR 1973

INDEX OF PERFORMANCE FOR FLIR (FORWARD LOOKING INFRARED) IMAGING DEVICES (U)

PHASE REPORT
AIRTASK NO. A3605333/202B/2F00343604

UNCLASSIFIED

~~Distribution Limitation(s): 02 - U.S. GOVT. AND THEIR CONTRACTORS~~

CLASSIFIED BY AIRTASK A3605333/202B/2F00343604
SUBJECT TO GENERAL DECLASSIFICATION
SCHEDULE OF EXECUTIVE ORDER 11652
DECLASSIFIED ON 31 DECEMBER 1979

Change Authority: *C TO U GDS*

~~CONFIDENTIAL~~

[redacted] UNCLASSIFIED

DEPARTMENT OF THE NAVY
NAVAL AIR DEVELOPMENT CENTER
WARMINSTER, PA. 18974

Aero-Electronic Technology Department

REPORT NO. NADC-72167-AE

10 April 1973

INDEX OF PERFORMANCE FOR FLIR (FORWARD LOOKING INFRARED) IMAGING DEVICES (U)

PHASE REPORT
AIRTASK NO. A3605333/202B/2F00343604

A certain combination of the FLIR performance parameters of resolution, sensitivity, field of view and frame rate is defined as the "index of performance" and is related by a tradeoff equation to FLIR construction parameters such as diameter of the collecting optics and the number of infrared detectors. Graphs illustrating the use of the equation for analyzing the performance of FLIR equipments and exploring design tradeoffs are given. The indices of performance of past and present FLIR devices are used to trace the progress of FLIR development and to extrapolate into the future. (U)

Reported by: (b)(6)
P. M. Moser N. E. MacMeekin
Applied Research Division

Approved by: (b)(6)
Superintendent
Applied Research Division

(b)(6)
Deputy Director, Acting

Distribution Limitation(s):
~~02 - U.S. GOVT. AND THEIR CONTRACTORS~~

Change Authority: C TO U GDS

[redacted] UNCLASSIFIED

UNCLASSIFIED
Security Classification

DOCUMENT CONTROL DATA - R & D

Security classification of title, body of abstract and indexing annotation must be entered when the overall report is classified)

1. ORIGINATING ACTIVITY (Corporate author)

AERO-ELECTRONIC TECHNOLOGY DEPARTMENT
NAVAL AIR DEVELOPMENT CENTER
WARMINSTER, PENNSYLVANIA 18974

2a. REPORT SECURITY CLASSIFICATION

[redacted]

2b. GROUP

*

3. REPORT TITLE

INDEX OF PERFORMANCE FOR FLIR (FORWARD LOOKING INFRARED) IMAGING DEVICES (U)

4. DESCRIPTIVE NOTES (*Type of report and inclusive dates*)

PHASE REPORT

5. AUTHOR(S) (*First name, middle initial, last name*)

P. M. MOSER
N. E. MACMEEKIN

6. REPORT DATE

10 APRIL 1973

7a. TOTAL NO. OF PAGES

25

7b. NO. OF REFS

8a. CONTRACT OR GRANT NO.

b. PROJECT NO.

AIRTASK NO. A3605333/202B/2F00343604

c.

d.

9a. ORIGINATOR'S REPORT NUMBER(S)

NADC-72167-AE

9b. OTHER REPORT NO(S) (*Any other numbers that may be assigned this report*)

10. DISTRIBUTION STATEMENT

11. SUPPLEMENTARY NOTES

12. SPONSORING MILITARY ACTIVITY

NAVAL AIR SYSTEMS COMMAND
DEPARTMENT OF THE NAVY

13. ABSTRACT

A certain combination of the FLIR performance parameters of resolution, sensitivity, field of view and frame rate is defined as the "index of performance" and is related by a tradeoff equation to FLIR construction parameters such as diameter of the collecting optics and the number of infrared detectors. Graphs illustrating the use of the equation for analyzing the performance of FLIR equipments and exploring design tradeoffs are given. The indices of performance of past and present FLIR devices are used to trace the progress of FLIR development and to extrapolate into the future. (U)

* *Classified by AIRTASK A3605333/202B/2F00342604; SUBJECT TO GENERAL DECLASSIFICATION; SCHEDULE OF EXECUTIVE ORDER 11652; DECLASSIFIED ON 31 DECEMBER 1979.*

14. KEY WORDS	LINK A		LINK B		LINK C	
	ROLE	WT	ROLE	WT	ROLE	WT
INFRARED						
FORWARD LOOKING						
IMAGING						
ATTACK AIRCRAFT						

S U M M A R Y

INTRODUCTION

(U) Under AIRTASK A3605333/202B/2F00343604 the NAVAIRDEVCEN is performing operational and system analyses and state-of-the-art technology surveys and projections as a first effort in the development of FLIR (forward looking infrared) imaging devices that would be affordable in large quantities and optimized for the missions of single-place attack aircraft.

(U) This report explores the tradeoffs of FLIR performance parameters for weight, complexity and cost, and traces quantitatively the historical development of FLIRs in a manner that permits an extrapolation into the future.

SUMMARY OF RESULTS

(U) Mathematical expressions are derived for FLIR signal-to-noise ratio and noise equivalent temperature difference. The latter equation is then recast by separating the FLIR performance parameters from the construction parameters to provide a tradeoff equation whose use is illustrated by means of a nomograph. The combination of performance parameters that appears in the tradeoff equation is then defined as the "index of performance." Indices of performance of FLIRs developed since 1964 are tabulated and values of the common logarithm of the ratio of index of performance and weight are plotted as a function of the year of development. The resulting graph not only illustrates the upward trend in the FLIR state of the art but also enables one to estimate weights of future equipments of any given index of performance. Index of performance is then related to FLIR complexity and cost. A family of curves of minimum resolvable temperature difference as a function of spatial frequency/target apparent size is presented and discussed for four hypothetical FLIRs having equal indices of performance.

CONCLUSIONS

(U) This report provides means for analyzing the performance of FLIR equipments and for investigating the tradeoffs available in the design of a FLIR of any given weight and complexity. Index of performance, as defined herein, appears to be a useful concept for assessing the state of the art and for predicting future development trends. As with any single-number figure of merit used to describe complex equipments performing complex tasks, index of performance should be used as an indicator rather than as a proof of equipment quality.

TABLE OF CONTENTS

LIST OF TABLES

LIST OF FIGURES

EXPLANATION OF SYMBOLS

(U) In this discussion the following symbols, some of which are further described in figure 1, are used:

S/N	Ratio of the peak signal voltage to the root-mean-square noise voltage of an infrared detector. (dimensionless)
D^*_{av}	Average spectral detectivity of an infrared detector over the spectral range of interest. "Detectivity" is equal numerically to the signal-to-noise ratio measured over a 1-Hz bandwidth for a detector having a sensitive area of one square centimeter when subjected to a change in incident radiant power of 1 watt. (cm $Hz^{1/2}$/watt)
ΔP	Change in radiant power over the spectral range of interest incident on the infrared detector. (watt)
a	Sensitive area of an infrared detector. (cm^2)
Δf	Electrical bandwidth over which signal-to-noise ratio is measured. (Hz)
A	Area of the component normal to the detector viewing direction of a portion of a uniform-temperature radiating surface of a blackbody target viewed instantaneously by an infrared detector. (cm^2)
x	Range to the target from the FLIR collecting optics. (cm)
F	Focal length of the FLIR optical system. (cm)
ω	Instantaneous solid angular field of view of an infrared detector projected through the FLIR optical system. (steradian)
D	Effective aperture diameter of the FLIR collecting optics. (cm)
Ω	Solid angle subtended at the target by the FLIR collecting optics. (steradian)
ΔT	Difference in temperature of the portion of the target viewed by the infrared detector relative to the surrounding target area. (K°)
L	Variation in radiant power emitted by the target per square centimeter per kelvin degree variation in temperature corrected for atmospheric transmission losses, if any. (watt/$cm^2 \cdot K°$)
e_{op}	Efficiency of the FLIR optical system over the spectral range of interest. This factor takes into account transmission/reflection losses and obscuration in the optics chain. (dimensionless)
e_{sc}	Scanning efficiency. This factor is the fraction of the time, over a complete scan cycle, that the infrared detector is engaged in viewing the scene of interest. (dimensionless)

n	Number of infrared detectors in the scanning array. It is assumed that all of the detectors are equal in sensitive area and detectivity and that they all scan at an equal constant angular rate. (dimensionless)
ω'	Total solid angle scanned by all the detectors per frame. (steradian)
η	Scanning frame rate. (sec^{-1})
τ	Dwell time per detector per picture element. (sec)
NEΔT	Noise equivalent temperature difference. This is the difference in temperature of the target area viewed by a detector that produces a peak signal equal to the root-mean-square noise generated in the detector. (K°)
N	Number of picture elements per frame. (dimensionless)
N'	Number of picture elements scanned per second during the active imaging portion of the scan. (sec^{-1})
D^{**}_{av}	A normalization of D^*_{av} to account for the variation in D^*_{av} of a background radiation noise limited detector as a function of the solid angle over which it accepts radiation. (cm $Hz^{1/2}$/watt)
Ω'	Solid angle over which the detector accepts radiation. (steradian)
I	Index of performance of a FLIR set. $[(K° \ sec^{1/2} \ rad)^{-1}]$
f/no	Ratio of focal length F and diameter D. (dimensionless)
α	Nominal resolution of a FLIR. (radian) For a square detector $\alpha = \sqrt{\omega}$.
MRT	Minimum resolvable temperature difference. (C°)

DERIVATION OF FLIR PERFORMANCE EQUATIONS

(U) From the definition of D^*_{av},

$$S/N = \frac{D^*_{av} \ \Delta P}{a^{1/2} \ (\Delta f)^{1/2}} \ . \tag{1}$$

(U) The target area from which a single detector accepts radiation is

$$A = \omega x^2 = \frac{a \ x^2}{F^2} \ . \tag{2}$$

(U) The solid angle subtended at the target by the FLIR collecting optics is

$$\Omega = \frac{\pi (D/2)^2}{x^2} \; . \tag{3}$$

(U) For a Lambertian radiator, the fraction of the power radiated normal to the target surface per steradian of solid angle Ω relative to the total radiated into a hemisphere is $1/\pi$.

Therefore,

$$\Delta P = \frac{1}{\pi} \; L A \Omega e_{op} \Delta T$$

$$= \frac{L \; a x^2 \; \pi D^2 \; e_{op} \Delta T}{\pi \; F^2 \quad 4x^2}$$

$$= \frac{a \; D^2 \; e_{op} \; L \; \Delta T}{4F^2} \; . \tag{4}$$

(U) The number of picture elements per frame is given by

$$N = \frac{\omega'}{\omega} \tag{5}$$

(U) The maximum rate at which picture elements are scanned is

$$N' = \frac{N \; \eta}{e_{sc}} = \frac{\eta \; \omega'}{\omega \; e_{sc}} \; . \tag{6}$$

(U) The required electrical bandwidth per detector is therefore

$$\Delta f = \frac{1}{2\tau} = \frac{N'}{2n} = \frac{\eta \omega'}{2n\omega e_{sc}} \; . \tag{7}$$

(U) Substituting equations (4) and (7) into equation (1) yields

$$S/N = \frac{D^*_{av} \; a \; D^2 e_{op} L \; \Delta T \sqrt{2} \; n^{1/2} \; \omega^{1/2} \; e_{sc}{}^{1/2}}{a^{1/2} \qquad 4F^2 \qquad \eta^{1/2} \qquad \omega'^{1/2}}$$

$$= \frac{D^*_{av} \; D^2 e_{op} L \; \Delta T \; n^{1/2} \; a^{1/2} \; \omega^{1/2} \; e_{sc}{}^{1/2}}{2\sqrt{2} \quad F^2 \qquad \eta^{1/2} \qquad \omega'^{1/2}}$$

(U) Since $a^{1/2}/F = \omega^{1/2}$,

$$S/N = \frac{D^*_{av} \; D^2 \; e_{op} \; L\Delta T \; n^{1/2} \; \omega e_{sc}{}^{1/2}}{2\sqrt{2}\; F \qquad \eta^{1/2} \qquad \omega'^{1/2}}$$

(U) For S/N = 1, ΔT = NEΔT

and

$$2\sqrt{2}\; F \; \eta^{1/2} \; \omega'^{1/2} = D^*_{av} \; D^2 \; e_{op} \; n^{1/2} \; \omega e_{sc}{}^{1/2} \; L \; (NE\Delta T). \qquad (8)$$

Therefore

$$NE\Delta T = \frac{2\sqrt{2}\; F \; \eta^{1/2} \; \omega'^{1/2}}{D^*_{av} \; D^2 \; e_{op} \; e_{sc}{}^{1/2} \; n^{1/2} \; \omega L} \; . \qquad (9)$$

Equation (9) is of value in analyzing the performance of FLIR equipments.

(U) The factors in equation (8) can be regrouped such that equipment performance parameters are displayed on the left and equipment design parameters are displayed on the right. That is,

$$\frac{\eta^{1/2} \; \omega'^{1/2}}{(NE\Delta T) \; \omega} = D^*_{av} \frac{D^2}{F} \; n^{1/2} \; e_{sc}{}^{1/2} \; e_{op} \frac{L}{2\sqrt{2}} \; . \qquad (10)$$

The left side of equation (10) is defined as the FLIR index of performance I.

(U) Since D/F = 1/f/no,

$$I = \frac{\eta^{1/2} \; \omega'^{1/2}}{(NE\Delta T) \; \omega} = \frac{D^*_{av} \; D \; n^{1/2} \; e_{sc}{}^{1/2} \; e_{op} \; L}{2\sqrt{2} \quad f/no} \; . \qquad (11)$$

(U) For a square detector

$$I = \frac{\eta^{1/2} \; \omega'^{1/2}}{(NE\Delta T) \; \alpha^2} = \frac{\eta^{1/2} \; N^{1/2}}{(NE\Delta T) \; \alpha} = \frac{D^*_{av} \; D \; n^{1/2} \; e_{sc}{}^{1/2} \; e_{op} \; L}{2\sqrt{2} \quad f/no} \; . \qquad (12)$$

(U) For the special case of a background radiation noise limited detector

$$D^{**}_{av} = \left(\frac{\Omega'}{\pi}\right)^{1/2} D^*_{av} \; .$$

(U) If the detector is cold-shielded in such a manner that it receives radiation from only the FLIR optical system

$$\Omega = \frac{\pi D^2}{4 F^2} = \frac{\pi}{4 (f/no)^2},$$

$$D^{**}_{av} = \left(\frac{\pi}{4\pi (f/no)^2}\right)^{1/2} D^*_{av} = \frac{1}{2 f/no} D^*_{av}$$

and

$$D^*_{av} = 2 f/no\, D^{**}_{av} . \tag{13}$$

(U) Substituting equation (13) into equation (11) yields, for the background radiation noise limited case,

$$I = \frac{n^{1/2} \omega'^{1/2}}{(NE\Delta T) \omega} = \frac{D^{**}_{av} D n^{1/2} e_{sc}^{1/2} e_{op} L}{\sqrt{2}} . \tag{14}$$

(U) In general, the greater its value of I, the better a FLIR will perform. The right side of equations (11), (12) or (14) indicates the price that must be paid for performance in terms of size (D) and complexity (n) of the equipment. The values of the efficiency factors (e_{sc} and e_{op}) are largely determined by the ingenuity of the optical design engineer and may have values ranging from about 0.5 to 1.0. As a rule of thumb, the simpler the scanner, the easier it is to achieve values of these efficiencies approaching unity. Both D^*_{av} and L are wavelength dependent and should be reckoned over the same band. It is desirable to maximize the product LD^*_{av}; inasmuch as D^*_{av} for a detector can be increased by decreasing (by cold-filtering) the wavelength interval over which it responds and L decreases with decreasing spectral bandwidth, it is necessary to select an optimum compromise for the spectral bandwidth.

(U) Values of L have been computed with the aid of a General Electric Radiation Calculator by effectively differentiating Planck's radiation formula with respect to temperature and integrating the resulting function over various wavelength intervals. Values of L corresponding to variations in a 15° C blackbody target are given in table I. These values are appropriate for use in calculating FLIR performance under laboratory conditions insofar as atmospheric transmission losses have been disregarded.

(U) For calculations of performance under field conditions, the value of L must be reduced to reflect atmospheric transmission losses. If it is assumed that the only significant losses result from water vapor absorption, values of L as a function of the length of the column of precipitable water in the path from the sensor to the target can be calculated rather easily. The spectral transmission curves corresponding to the various amounts of precipitable water are multiplied point-by-point by the spectral radiant emittance temperature derivative curve, and the resultant curves are integrated over the wavelength band of interest. Such calculations have been carried out for the 8.0- to 12.5-μm band for blackbody target temperature variations about 15° C, and the results are summarized in table II.

TRADEOFF EQUATION

(U) Equation (12) can be regarded as a tradeoff equation which relates FLIR performance characteristics to FLIR design/construction characteristics; i.e.,

$$I = \frac{\eta^{1/2}\,\omega'^{1/2}}{(NE\Delta T)\,\alpha^2} = \frac{D^*_{av}\,D\,n^{1/2}\,e_{sc}^{1/2}\,e_{op}}{f/no}\;\frac{L}{2\sqrt{2}}\,. \qquad (15)$$

(U) The parameters on the right side of this equation over which the FLIR designer has the greatest control are D, the diameter of the collecting optics, and n, the number of detector elements. The volume and weight of the FLIR might be expected to vary as D raised to a power of two to three and the system complexity to increase with increasing n. Therefore, it does not seem unreasonable to assume that, at any given point in time, the cost of a FLIR would be a function of its index of performance. If one has fixed resources, one can afford to purchase a FLIR of some given index of performance; it then remains for the buyer to choose the affordable combination of η, ω', NEΔT, and α that is optimum for the mission to be performed.

(U) Equation (15) can be simplified by selecting fixed numerical values for those parameters over which one has little control and/or over which variations are likely to be relatively small. For purposes of discussion assume the following values:

η = 30 frames/sec

$\frac{\omega'}{\alpha^2} = \frac{\omega'}{\omega} = N = 8 \times 10^4$ picture elements/frame. (This corresponds, for example, to a 200- by 400-element picture.)

$D^*_{av} = 1.6 \times 10^{10}$ cm $Hz^{1/2}$/watt

$e_{sc} = 0.6$

$e_{op} = 0.8$

$f/no = 2.0$

$L = 1.92 \times 10^{-4}$ watt/$cm^2 \cdot K°$.

(U) If these values are inserted into equation (15), one obtains

$$I = \frac{30^{1/2} \times (8 \times 10^4)^{1/2}}{(NE\Delta T)\ \alpha} = \frac{1.6 \times 10^{10} \times 0.6^{1/2} \times 0.8 \times 1.92 \times 10^{-4}\ Dn^{1/2}}{2.0 \times 2\sqrt{2}}$$

or

$$I = \frac{1.55 \times 10^3}{(NE\Delta T)\ \alpha} = 3.37 \times 10^5\ Dn^{1/2}. \qquad (16)$$

If α is expressed in milliradians and D in inches, equation (16) can be written as

$$I = \frac{1.55 \times 10^6}{(NE\Delta T)\ \alpha} = 8.55 \times 10^5\ Dn^{1/2}. \qquad (17)$$

(U) Equation (17) is expressed in the form of a nomograph in figure 2. Subject to the foregoing assumptions, one can use this nomograph to explore the various tradeoff possibilities and to interrelate the performance parameters of nominal resolution and noise equivalent temperature difference, the design parameters of aperture diameter and number of detector elements, and index of performance.

(U) In the foregoing it has been tacitly assumed that the diameter of the collecting optics is sufficiently large that the system resolution is not seriously limited by diffraction. If the minimum aperture diameter D_{min} of the optics is selected such that the angular diameter of the Airy disk resulting from diffraction of the radiation as it passes through the aperture equals the detector angular subtense,

$$D_{min} = 2.44\ \lambda/\alpha. \qquad (18)$$

Plots of equation (18) for the case of $\lambda = 10\ \mu m$ are given in figure 3.

(U) If equations (12) and (14) are compared, it is seen that if background radiation noise limited detectors are used, the performance of the FLIR is independent of the system f/no, whereas for the non-background limited case, index of performance varies inversely as the f/no. This permits greater flexibility of design in the former case, as compared to the latter, by allowing the use of relatively slow optics and the attendant advantages of greater depth of field, reduced criticality of focusing, greater ease of fabricating the optical system, and reduced cost of the optical elements. Unfortunately, some of the more desirable detectors (such as mercury cadmium telluride) do not operate in the background radiation noise limited condition when viewing terrestrial scenes unless they accept radiation from a large solid angle which, in turn, implies a fast optical system.

RATIOS OF INDEX OF PERFORMANCE TO WEIGHT

(U) Indices of performance for 57 frame-scanning, real-time, passive infrared imaging devices have been calculated by inserting available published data into the FLIR performance portion of equation (11)

$$I = \frac{\eta^{1/2}\ \omega'^{1/2}}{(NE\Delta T)\ \omega} .$$

In most cases these data are design performance figures rather than laboratory measured values. These indices of performance and the data upon which they are based are summarized in chronological order in table III. This table also lists the weight of each equipment, the ratio of index of performance and weight, and the common logarithm of this ratio. In certain cases the weights were "normalized." For example, some of the sets are furnished with two displays, whereas others are designed to operate with independent multipurpose displays. In such cases, the weights were adjusted to allow for a single display.

U ~~(C)~~ In figure 4, values of the common logarithm of the ratio of index of performance to weight for each of the 57 infrared imaging devices are plotted as a function of the contract date (or other identifiable starting date) for the construction of the equipment. In some cases, only the year of the contract could be determined; in such situations the points are plotted at the midpoints of the corresponding calendar years. In one case, two of the plotted points coincide; accordingly the number of plotted points appears to be less than 57. Although there is considerable scattering of the plotted points, there does appear to be an upward trend in FLIR performance-to-weight ratios. A least-squares straight-line fit to the plotted points indicates that FLIR performance-to-weight ratios are improving by a factor of ten every 4.3 years.

U (~~C~~) With a proper amount of caution, figure 4 can be applied to a number of ends. For example, it establishes a value of 6.22×10^5 as the June 1972 state-of-the-art value for FLIR performance-to-weight ratios. If this number is applied to the data given in figure 2, one can relate various combinations of FLIR resolution and sensitivity to equipment weight by simply dividing the corresponding values of index of performance I by 6.22×10^5. This procedure was employed in arriving at the scale of "weight" in figure 2.

U (~~C~~) To illustrate the use of the nomograph, consider a 0.25-mrad FLIR having an NEΔT of 0.25 C°. Its index of performance would be 24.8×10^6 and, if a contract had been awarded for its development in the middle of calendar year 1972, it could have been built into a 39.9-lb package. It could achieve this index of performance with, as examples, a 50-element detector array and a 4.1-inch diameter optical system or a 25-element detector array and a 5.8-inch diameter optical system. If one carries this reasoning one step further and assumes that, in production, military avionic equipments cost $1,000 per pound, it can then be inferred that the FLIR cited as an example would sell at a unit cost of $39,900. In a similar manner, one can use the nomograph of figure 2 to infer other possible combinations of FLIR weight, cost, and performance.

(U) Another application of the graph of figure 4 is to determine the relative standing of the various FLIRs with respect to the "norm" line. It may prove to be a worthwhile exercise to investigate the attributes of the various FLIRs as a function of whether they fall below or above the norm. If this question is approached in a somewhat cynical manner, one observes, among other things, that proposed equipments or those in the conceptual stage tend to fall above the norm, and those that have been translated into hardware tend to fall below the norm. In the painful transition from concept to hardware, performance seems to decrease while weight increases.

(U) Still another application of the graph of figure 4 is the prediction of future performance-to-weight ratios. Suppose, for example, one wants to develop a FLIR for use in an aircraft that will first appear in the year 1976. By allowing an appropriate amount of time for development and fabrication, one can forecast the capabilities of a FLIR that would be deliverable in time to be fitted into the aircraft.

INDEX OF PERFORMANCE AND MINIMUM RESOLVABLE TEMPERATURE DIFFERENCE

(U) It should not be concluded from the foregoing that for any arbitrary mission all FLIRs of given index of performance will perform equally. One can see from equation (12) and also from figure 2, that for a given index of performance an infinity of combinations of $NE\Delta T$ and α is possible. One can further convince himself that for a particular mission (and I = constant) there is an optimum combination of $NE\Delta T$ and α. This follows from the argument that both combinations of infinite $NE\Delta T$ and zero α and of infinite α and zero $NE\Delta T$ would be useless, but that combinations of intermediate values are useful. Some insight into the tradeoffs that are possible can be gained by recognizing that for a given FLIR equipment "resolution" and "sensitivity" are not independent constant quantities but that one is a function of the other. This relationship is nicely expressable in terms of a plot of minimum resolvable temperature difference as a function of target spatial frequency. (For purposes of MRT determination, target spatial frequency - in cycles/mrad - is the reciprocal of twice the angle subtended at the sensor by the narrow dimension of each bar of a "standard" 4-bar target, each bar of which has a 7-to-1 length-to-width ratio.) Simply stated, the temperature contrast required for a particular FLIR equipment to resolve the target bars depends on the size of the bars; conversely, the resolution yielded by a FLIR depends on the thermal contrast of the target bars.

(U) Figure 5 is a family of MRT curves for several hypothetical FLIRs having equal indices of performance but different combinations of $NE\Delta T$ and α. Of special interest in this figure are the intersections of the curves. For example, for resolving bars subtending an angle of 0.48 mrad (corresponding to a spatial frequency of 1.05 cycles/mrad), equal performance can be achieved by both a 0.25-mrad FLIR and a 0.125-mrad FLIR provided the products of $NE\Delta T$ and α for each are equal. For resolving bars subtending angles greater than 0.48 mrad, the 0.25-mrad FLIR would outperform the 0.125-mrad equipment, whereas the opposite would be true if bars subtending angles of less than 0.48 mrad are to be resolved. Another interpretation of the foregoing is that for target thermal contrasts less than 0.24 C°, the 0.25-mrad FLIR yields better spatial resolution than the 0.125-mrad equipment.

CONCLUDING REMARKS

(U) This is the first of a series of reports dealing with FLIRs in general and with low cost FLIRs for use in Navy single-place attack aircraft in particular. In a subsequent report, a mathematical model of FLIR performance will be described which will permit relating the FLIR design characteristics of nominal resolution and noise equivalent temperature difference to target acquisition, classification, and identification ranges. In a third report, FLIR range requirements will be established in terms of various aircraft altitudes and speeds, weapon types, and methods of delivery. The information contained in this series of reports should permit a judicious choice of design characteristics for an optimum low cost FLIR for use in single-place attack aircraft.

TABLE I

VALUES OF THE VARIATION L IN RADIANT EMITTANCE PER KELVIN DEGREE VARIATION IN BLACKBODY TARGET TEMPERATURE FOR VARIOUS WAVELENGTH INTERVALS (T = 15° C)

Wavelength Interval (μm)	L (watt/cm^2·K°)
8.0 - 11.5	1.54×10^{-4}
8.0 - 12.0	1.71×10^{-4}
8.0 - 12.5	1.92×10^{-4}
8.0 - 13.0	2.04×10^{-4}
8.0 - 13.5	2.25×10^{-4}
8.5 - 11.5	1.30×10^{-4}
8.5 - 12.0	1.47×10^{-4}
8.5 - 12.5	1.68×10^{-4}
8.5 - 13.0	1.80×10^{-4}
8.5 - 13.5	2.01×10^{-4}

TABLE II

VALUES OF THE VARIATION L IN RADIANT EMITTANCE PER KELVIN DEGREE VARIATION IN BLACKBODY TARGET TEMPERATURE FOR THE WAVELENGTH INTERVAL 8.0 TO 12.5 μm FOR VARIOUS AMOUNTS OF PRECIPITABLE WATER IN THE TRANSMISSION PATH (T=15°C)

Water Vapor in Path (cm of precipitable water)	L (watt/cm^2·K°)
1.0	155×10^{-6}
2.0	137×10^{-6}
5.0	99.8×10^{-6}
10	65.4×10^{-6}
20	34.9×10^{-6}
50	7.0×10^{-6}
100	0.8×10^{-6}

CONFIDENTIAL

TABLE III

SUMMARY OF CHARACTERISTICS OF FORWARD LOOKING INFRARED DEVICES (U)

Contract/ Start Date	Manufacturer	Equipment Name	NFOV	IFOV (mrad)	NEAT (C°)	Frame Rate (f/sec)	Index of Performance	Weight (lb)	1/W	$\log_{10}$ 1/W
8/64	TI	FLIR 103A (Feasibility Model)	20°x40°	2.0	0.6	24	1.01×10^{6}	214	4.70×10^{3}	3.67
8/64	TI	FLIR 103C (Feasibility Model)	20°x40°	1.0	1.7	12	1.01×10^{6}	214	4.70×10^{3}	3.67
8/64	TI	FLIR 106A (Feasibility Model)	20°x40°	2.0	0.4	24	1.51×10^{6}	214	7.08×10^{3}	3.85
8/64	TI	FLIR 106C (Feasibility Model)	20°x40°	1.0	1.2	12	1.43×10^{6}	214	6.69×10^{3}	3.82
6/65	TI	FL-28	20°x40°	1.5	0.3	22	3.42×10^{6}	439	7.79×10^{3}	3.89
6/65	Raytheon	FIORD	6.5°x12°	0.5	0.5	10	3.86×10^{6}	36	1.07×10^{5}	5.03
9/65	TI	FLIR 306A (Dual-Spectrum)	20°x40°	2.0	0.8	24	7.55×10^{5}	381	1.98×10^{3}	3.30
9/65	TI	FLIR 430B (Airborne View-finder)	20°x40°	1.5	0.4	30	3.02×10^{6}	243	1.24×10^{4}	4.09
1/66	TI	FLIR 1288 (Feasibility Follow-on)	20°x40°	1.5	0.4	27.5	2.88×10^{6}	240	1.21×10^{4}	4.08
3/66	TI	FLIR 2308 (Lonesome Tiger)	20°x40°	1.5	0.3	30	4.03×10^{6}	274	1.47×10^{4}	4.17
3/66	TI	FLIR 230C (Lonesome Tiger)	20°x40°	1.0	0.5	30	5.44×10^{6}	274	1.98×10^{4}	4.30
5/66	TI	FLIR 6308 (8-52)	20°x40°	1.5	0.5	30	2.42×10^{6}	266	9.11×10^{3}	3.96
6/66	TI	Dual FLIR	20°x40°	1.5	0.3	30	4.03×10^{6}	118	3.42×10^{4}	4.53
6/66	TI	FLIR 8308 (TRIM)	20°x40°	1.5	0.35	26	3.20×10^{6}	289	1.11×10^{4}	4.04
6/66	Navy	ADAM	12.4°x80°	1.0	0.03	14	6.09×10^{7}	425	1.43×10^{5}	5.16
8/66	TI	FLIR 530C (Blackspot)	12°x32°	1.5	0.6	30	1.39×10^{6}	266	5.23×10^{3}	3.72
11/66	AVCO	MIRTAS	12°x45°	1.0	0.2	30	1.11×10^{7}	127	8.75×10^{4}	4.94
12/66	Aerojet	ADFLIR (AAQ-5, C19)	5°x7.5°	0.25	0.3	30	3.14×10^{7}	425	7.39×10^{4}	4.87
6/67	Hughes	AN/AAS-29	5°x6.7°	0.25	0.3	30	2.95×10^{7}	280	1.16×10^{5}	5.05
6/67	Hughes	AD FLIR (AFLIR)	5°x10°	0.25	0.25	30	4.34×10^{7}	299	1.45×10^{5}	5.16
6/67	Hughes	EVE FLIR	12.4°x40°	0.75x1.0	0.05	15	4.00×10^{7}	540	7.41×10^{4}	4.87
6/68	AVCO	AFR-500 (IRNS)	12°x45°	1.0	0.15	30	1.48×10^{7}	156	9.49×10^{4}	4.98
6/68	BOFORS	IR-Camera	12.5°x25°	1.2	0.10	4	4.28×10^{6}	90	4.76×10^{4}	4.68
6/68	Honeywell	FIRTI	2°x5°	0.25	0.3	15	1.14×10^{7}	739	1.54×10^{4}	4.19
6/68	Honeywell	Nightscope	5.7°x5.7°	1.0	0.2	25	2.48×10^{6}	12	2.06×10^{5}	5.31
6/68	PBEC	Lightweight Weapon Sight	3°x7°	0.5	0.4	15	3.10×10^{6}	8	3.88×10^{5}	5.59
6/68	Raytheon	Short Range Viewer	6.5°x12°	0.2	0.27	15	5.47×10^{5}	8	6.85×10^{4}	4.84
6/68	Hughes	NOD-LR-TI	2°x5°	0.25	0.15	15	2.28×10^{7}	49	4.65×10^{5}	5.67
6/68	Hughes	Short Range Viewer	6°x12°	0.2	0.35	15	4.08×10^{5}	5.3	7.72×10^{4}	4.89
late/68	Hughes	PINE (AN/AAS-25)	5°x6.7°	0.25	0.17	30	5.24×10^{7}	198	2.65×10^{5}	5.42
10/68	TI	AN/AAD-4 (FL-3)	5.5°x7.3°	0.33	0.18	15	2.18×10^{7}	441	4.95×10^{4}	4.69
4/69	TI	AN/AAS-26 (FL-22 Westing-house)	5.6°x7.5°	0.33	0.2	25	2.59×10^{7}	220	1.18×10^{5}	5.07
5/69	TI	AN/AAS-28 (FL-23, TRIM)	4°x5.3°	0.25	0.23	22.5	2.42×10^{7}	229	1.09×10^{5}	5.04
6/69	Aerojet	C3S FLIR	5°x7.5°	0.25	0.30	30	3.14×10^{7}	225	1.39×10^{5}	5.14
6/69	PBEC	AN/PAS-7 (Viewer)	6°x12°	2.0	0.4	15	3.58×10^{5}	5.2	6.89×10^{4}	4.84
6/69	PBEC	AN/VAS-1-(U) (FIRTI II)	4°x10°	0.34	0.3	15	1.24×10^{7}	370	3.36×10^{4}	4.53
6/69	TI	FL-30	5°x6.7°	0.25	0.25	30	3.56×10^{7}	140	2.54×10^{5}	5.40
6/69	AVCO	Blackspot	12°x20°	0.5x0.68	0.38	30	1.15×10^{7}	150	7.67×10^{4}	4.88
6/69	Hughes	EVS (B-52)	5°x6.7°	0.25	0.17	30	5.24×10^{7}	198	2.65×10^{5}	5.42
6/69	Hughes	HAFLIR	2.5°x3.3°	0.125	0.25	30	7.10×10^{7}	325	2.18×10^{5}	5.34
10/69	TI	OR-89/AA (S-3A FLIR)	5°x6.7°	0.25	0.25	30	3.56×10^{7}	281	1.27×10^{5}	5.10
3/70	AVCO	TOD	4°x10°	1.0	0.1	20	5.01×10^{6}	13	3.85×10^{5}	5.58
3/70	AGA	Thermovision System 680	10°x10°	1.3	0.123	16	2.83×10^{6}	82	3.46×10^{4}	4.54
6/70	TI	FS-2	12°x20°	1.0	0.25	40	6.85×10^{6}	40	1.71×10^{5}	5.23
6/70	Honeywell	FLIR	4.5°x4.5°	0.15	0.15	30	1.28×10^{8}	175	7.32×10^{5}	5.86
6/70	Hughes	PINE (NOGS)	5°x6.7°	0.25	0.17	30	5.24×10^{7}	343	1.53×10^{5}	5.18
6/70	AVCO	TDS	1° circular	0.08	0.2	30	6.61×10^{7}	148	4.46×10^{5}	5.66
7/70	TI	AN/AAD-6	5.6°x7.5°	0.33	0.2	30	2.85×10^{7}	441	6.46×10^{4}	4.81
9/70	AVCO	AVTDS	0.8° circular	0.06	0.15	30	1.11×10^{8}	140	7.94×10^{5}	5.90
11/70	EOS	LATIS	5° circular	0.15x0.25	0.25	30	4.55×10^{7}	178	2.50×10^{5}	5.40
1st qtr 71	TI	Austere FLIR	2.9° circular	0.125	0.1	15	1.12×10^{8}	120	9.34×10^{5}	5.97
1st qtr 71	Hughes	ATIS	4.5°x6°	0.25	0.11	15	5.10×10^{7}	70	7.29×10^{5}	5.86
2/71	TI	AN/AAS-28A	1.8°x2.4°	0.167	0.23	60	4.42×10^{7}	221	2.00×10^{5}	5.30
2nd qtr 71	TI	AN/AAD-7	2.25°x3°	0.167	0.15	30	6.00×10^{7}	440	1.37×10^{5}	5.14
6/71	Hughes	Discoid (NAVFLIR)	30°x62°	2.0	0.11	15	6.73×10^{6}	50	1.35×10^{5}	5.13
8/71	Dynarad	Thermal Imaging System	10°x10°	1.7	0.2	60	2.33×10^{6}	39	5.98×10^{4}	4.78
1/72	TI	SASI-modified OR-89/AA	1.4°x1.8°	0.133	0.15	60	8.05×10^{7}	300	2.68×10^{5}	5.43

CONFIDENTIAL

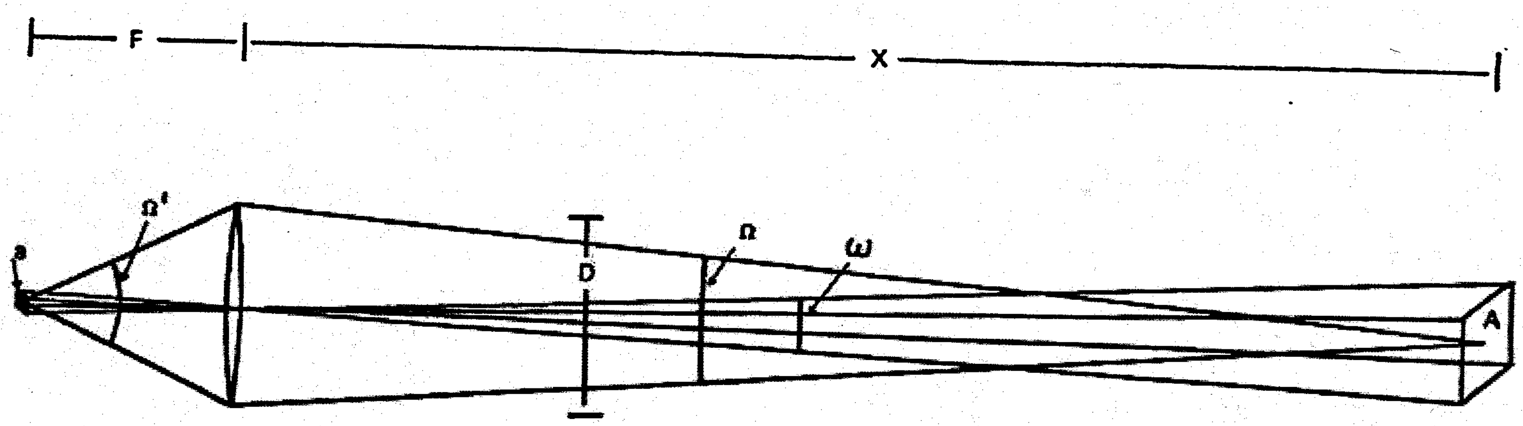

FIGURE 1 - Description of Geometrical Terms Used in Derivation of FLIR Performance Equations (U)

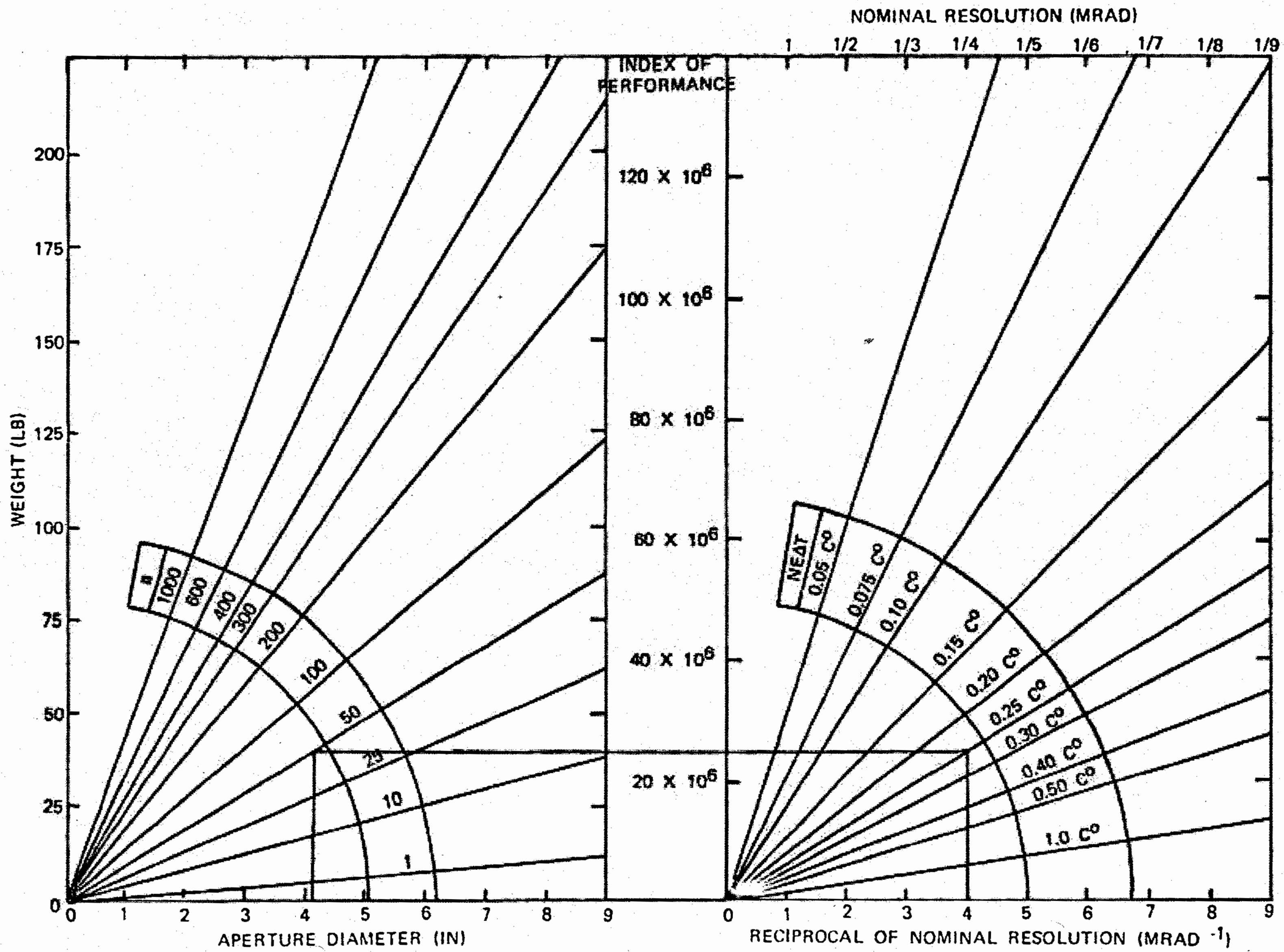

FIGURE 2 - Nomograph of FLIR Tradeoffs (U)

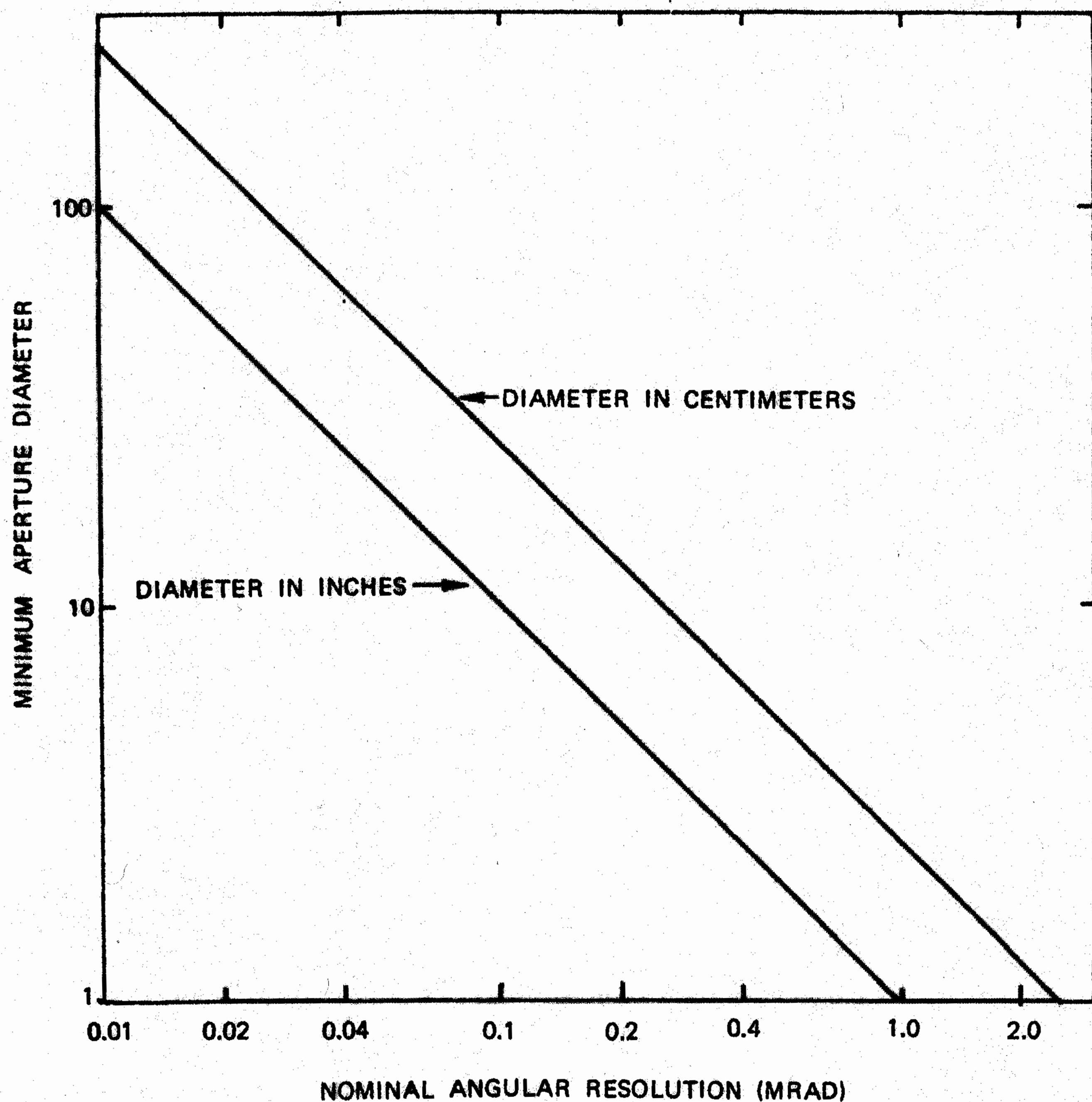

FIGURE 3 - Minimum Aperture Diameter For a Diffraction Limited FLIR as a Function of Required Resolution (U)

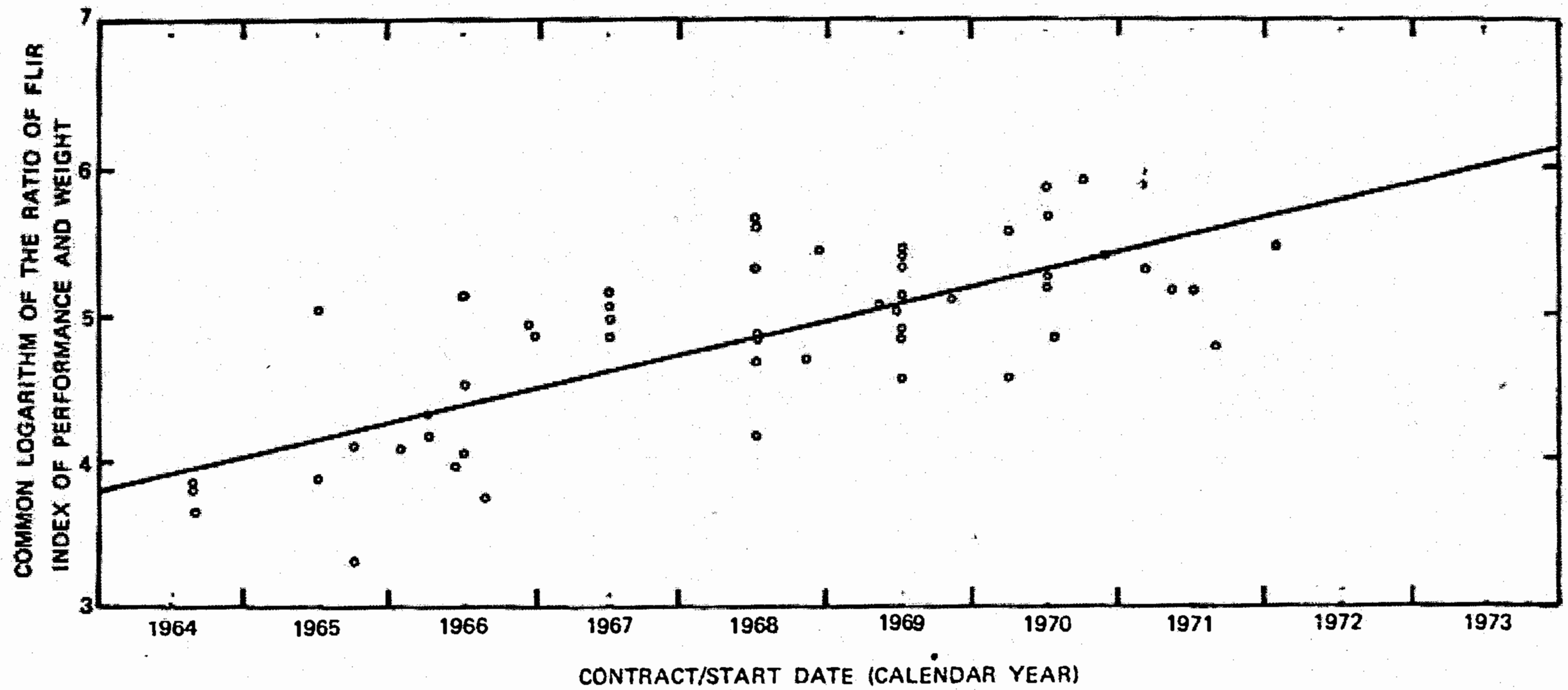

FIGURE 4 - FLIR Performance-to-Weight Ratios as a Function of Contract/Start Date (U)

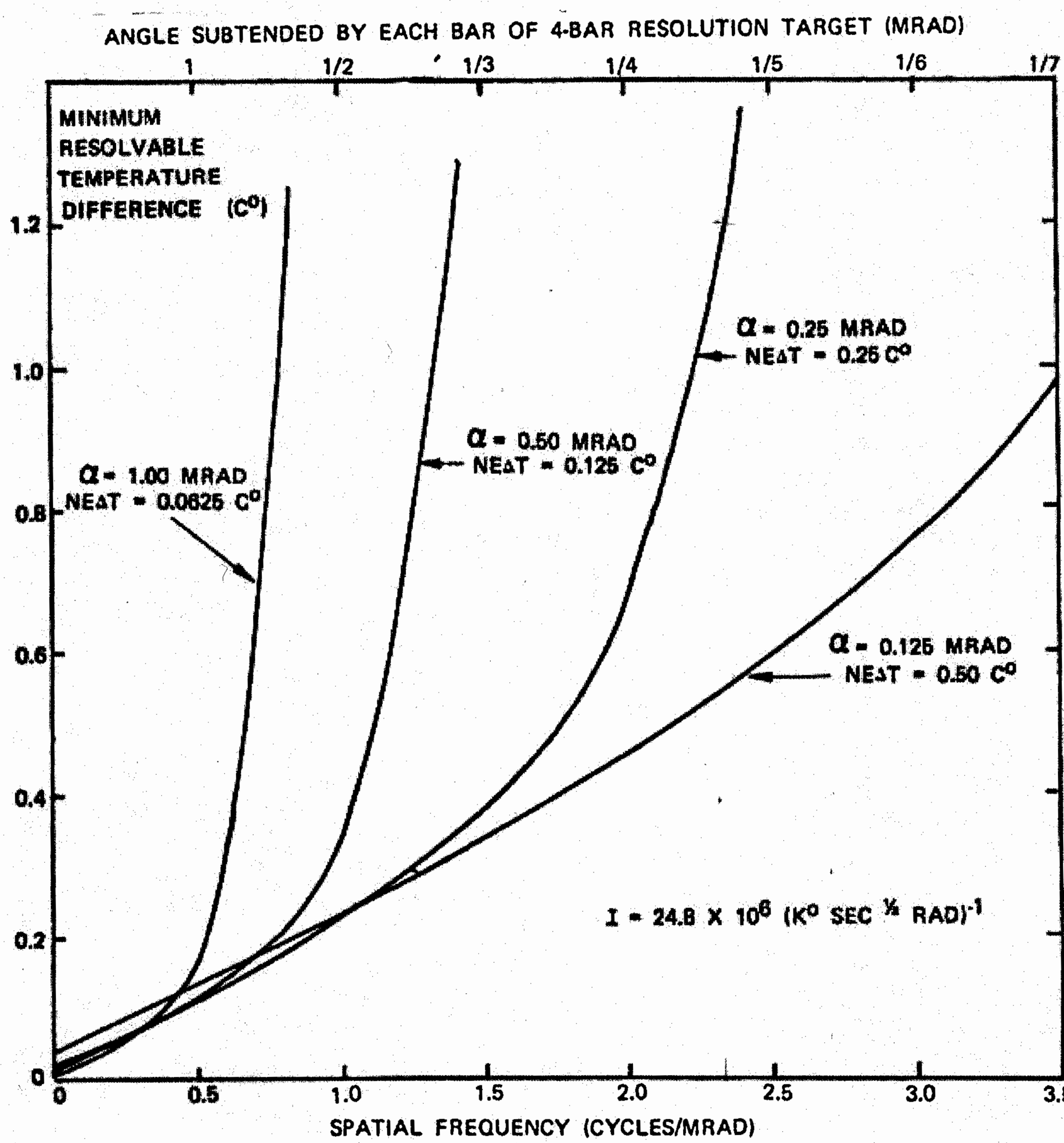

FIGURE 5 - Family of MRT Curves for Four Hypothetical FLIRs Having Equal Indices of Performance (U)

22 Feb 2017

MEMORANDUM FOR THE RECORD

FROM: Division Director EO & Special Mission Sensors, Avionics, Sensors and E* Warfare Dept (AIR 4.5.6)

TO: Office of Counsel, Naval Air Warfare Center, Aircraft Division (NAWCAD)

Subj: SECURITY RECOMMENDAION FOR FOIA REQUEST, DON FOIA CASE FILE NUMBER 2015-008952

Ref: (a) SECNAVINST 5720.42F, DON FOIA Program, 06 Jan 99

(b) Executive Order 13526

1. Releasable Recommendations. The following documents were reviewed by AIR 4.5.6. Each of the following documents were found to be releasable in their entirety:

   a. Document (1) of Subj. NAVAIRDEVCEN Report No. NADC-AW-L5902, 24 Mar 1959, “Investigation of a Towed-capsule Installation of the AN/ASH-2 Condensation Nuclei Detector” (ADB966296)
   b. Document (10) of Subj. NAVAIRDEVCEN Report No. NADC-AW-N6302, 4 Apr 1963, “Maritime Applications of Infrared Mapping Systems” (AD-359080L)
   c. Document (16) of Subj. NAVAIRDEVCEN Report No. NADC-AE-6759, 16 Jan 1968, “Modified Reconofax VI Infrared Mapping Set with Real Time Inflight Display” (AD-387513)
   d. Document (17) of Subj. NAVAIRDEVCEN Report No. NADC-AE-6828, 12 Nov 1968, “Modified AN/AAD-2(XE-2) Infrared Detecting Set with Real-Time Inflight Display (AD-500493)
   e. Document (18) of Subj. NAVAIRDEVCEN Report No. NADC-72167-AE, 10 Apr 1973, “Index of Performance for FLIR (Forward Looking Infrared) Imaging Devices” (AD-525116)

2. Partially Releasable Recommendations. AIR 4.5.6 recommends pages 27 through 68 are releasable the following report: Document (20) of Subj. Naval Research Laboratory Memorandum Report 3240, Proceedings of the Electro-Optics/Meteorology Meeting on 7 Aug 1975, Mar 1976 “FLIR Performance Modelling and its Dependence upon Climatology and Meteorology “(AD-D516929L). All other data in this report is not under the technical authority of AIR 4.5.6.

3. [redacted]

4. Basis of Recommendation. All information was reviewed with current class guides and what is considered open source information. Appropriate recommendations made above with respect to findings. Documents found with portions releasable were sanitized based on class guides and reference (b). Such disclosure of Department of the Navy classified information would give potential adversaries insight that would present a significant threat to national security.

5. Exemptions Utilized. Two separate exemptions were utilized in the determination of what information should be sanitized or exempted from release via Freedom of Information Act (FOIA) request process. All current Classified Military Information (CMI) has been sanitized out of the document under FOIA Exemption 1, Executive Order 13526 Section 3.3(4). This Executive Order Section covers CMI that was originally classified over 25 years ago from date of this memorandum. Subject matter experts within AIR 4.5.6 were utilized in making the exemption determinations.

6. Point of Contact. The point of contact for this security review and recommendation is Mr. Paul W. Reimel, AIR 4.5.6 Division Director, paul.reimel@navy.mil, 301-342-0100.

2/28/2017

X Paul W. Reimel

Paul W. Reimel

Signed by: REIMEL.PAUL.W.1229241016

Distribution:

NAWCAD 7.4

NAWCAD 4.5.6